



Pd nanoparticles immobilized on PAMAM-grafted MWCNTs hybrid materials as new recyclable catalyst for Mizoraki–Heck cross-coupling reactions

Mohammad Reza Nabid*, Yasamin Bide, Seyed Jamal Tabatabaei Rezaei

Department of Chemistry, Shahid Beheshti University, G.C., P.O. Box 1983963113 Tehran, Iran

ARTICLE INFO

Article history:

Received 21 May 2011

Received in revised form 10 August 2011

Accepted 16 August 2011

Available online 24 August 2011

Keywords:

Dendrimer

Palladium nanoparticles

Carbon nanotubes

Supported catalysis

Heck reaction

ABSTRACT

Polyamidoamine (PAMAM) dendrimers up to the third generation (G) were grown onto the surface of functionalized multiwall carbon nanotubes (MWCNTs-NH₂) by a divergent method, the PAMAM-grafted-MWCNTs (PAMAM-g-MWCNTs) hybrid materials were obtained. Because of the surface modification of the multiwall carbon nanotubes with PAMAM dendrimers, these hybrid materials are not only soluble in aqueous medium but also are able to trap water soluble metal ions such as Pd²⁺ via complex formation of PAMAM dendrimer with metal ions. The reduction of trapped palladium ions in the dendritic shell of PAMAM-g-MWCNTs by sodium borohydride led to immobilized palladium nanoparticles on the surface of MWCNTs. Thus, palladium nanoparticles were immobilized by PAMAM-g-MWCNTs hybrid materials (PdNs-PAMAM-g-MWCNTs) and their application as a new nanocatalyst toward Heck reaction in different conditions was investigated. The G3 and G2 hybrid materials were found to be very active in cross-coupling reactions of aryl iodides, bromides and also chlorides with olefinic compounds in Heck reactions with short reaction time duration and high yields. The catalyst can be recycled several times without loss in activity.

© 2011 Elsevier B.V. All rights reserved.

1. Introduction

Since their discovery by Iijima [1], carbon nanotubes (CNTs) have attracted great interest in the most fields of science due to their unique physical and chemical properties [2,3]. Owing to their unique structure and interesting properties such as large surface area, CNTs are excellent supporting materials for catalysts, especially in heterogeneous catalysis [4,5]. Although CNTs supported metal nanoparticles exhibit greater catalytic efficiency than their bulk counterparts, because of high surface-to-volume ratio [6], there are some difficulties in dispersing metal nanoparticles on the surface of pristine CNTs due to their hydrophobic nature as well as their tendency for agglomeration. In order to overcome these problems and to favor a high loading of nanoparticles, grafting well-defined polymers known as dendrimers can act as macromolecular coupling agents carrying multiple binding sites [7–16].

Dendrimers are nanosized, highly branched molecules, with very well-defined chemical structures, engineered precisely to carry molecules encapsulated in their interior void spaces or attached to their surface. These unique abilities of dendrimers led to the design of novel dendritic materials for a variety of advance applications [17]. Chemical attachment of dendrimers to

the surface of CNTs can be performed by either “convergent” or “divergent” methods. In convergent method prefabricated dendrimers are connected to functionalize CNTs through chemical reaction. The convergent synthesis strategy is characterized by low grafting density because of the hindrance of the dendrimer branches which react with CNTs [18–20]. The divergent method involves the growth of dendrimers from the surface of CNTs by first covalently attaching of appropriate functional groups. In contrast to convergent route this method leads to the higher grafting density and control over the dendrimer growth with the possibility of designable structures [21,22].

Palladium has been recognized as an indispensable catalyst for carbon–carbon and carbon–heteroatom bond forming reactions and there is a great deal of literature on its properties in many reactions [23–31]. Recently, palladium nanoparticles supported on insoluble solids have received considerable attention as a new generation of heterogeneous catalysts in various scientific fields because of their superior catalytic performance, good stability, ease of separation and satisfactory reusability in comparison to the traditional homogeneous Pd(OAc)₂, PdCl₂ catalysts [32–57]. Because of these reasons and also as a part of our ongoing research program on the application of catalysts for the development of useful new synthetic methodologies [58–61], herein, we report the synthesis of a heterogeneous palladium nanocatalyst supported on PAMAM-grafted-MWCNTs and its efficiency in the promotion of the Heck coupling reaction.

* Corresponding author. Tel.: +98 21 29902800; fax: +98 21 22431586.
E-mail address: m-nabid@sbu.ac.ir (M.R. Nabid).

Table 1
Amount of -NH_2 groups and Pd(0) on each generation of the PdNs-PAMAM-g-MWCNTs hybrid materials.

Entry	Generation	-NH_2 content ^a /mmol g ⁻¹	-NH_2 content ^b /mmol g ⁻¹	Amount of Pd(0) ^c /mmol g ⁻¹	Loading efficiency (%)
1	0	0.17	0.16	0.31	4.13
2	1	0.33	0.31	0.51	6.80
3	2	0.65	0.59	1.20	16.0
4	3	1.33	1.29	2.00	26.6

^a Determined by Titration method.

^b Determined by TGA.

^c Determined by AAS.

2. Experimental

2.1. Materials

The used MWCNTs were prepared by chemical vapor deposition procedure in the presence of Co/Mo/MgO as catalyst at 900 °C. The outer diameter of MWCNTs was between 20 and 40 nm. All solvents and reagents were purchased from Aldrich or Merck and used without further purification unless otherwise stated. 3-Azidopropylamine was prepared according to the reported procedures in relevant literature [62].

2.2. Instruments and characterization

¹H NMR spectra were recorded with a BRUKER DRX-300 AVANCE spectrometer, and D₂O or CDCl₃ were used as solvents. IR spectra were recorded on a Bomem MB-Series FT-IR spectrophotometer. Transmission electron microscopy (TEM) analyzes were performed by LEO 912AB electron microscope. XPS analysis was performed using a VG multilab 2000 spectrometer (ThermoVG scientific) in an ultra high vacuum. Catalysis products were analysed using a Varian 3900 GC (GC conversions were obtained using n-decane as an internal standard based on the amount of arylhalide employed relative to authentic standard product). Ultrasonic bath (EUROSONIC® 4D ultrasound cleaner with a frequency of 50 kHz and an output power of 350 W) was used to disperse materials in solvents. Thermogravimetric analysis (TGA) was carried out using STA 1500 instrument at a heating rate of 10 °C min⁻¹ in air. X-ray powder diffraction (XRD) data were collected on an XD-3A diffractometer using Cu K α radiation.

2.3. Preparation of amino functionalized MWCNTs

MWCNTs (2 g) were refluxed under stirring in the mixture of 1:3 (v/v) HNO₃ and H₂SO₄ at 90 °C for 24 h. The mixture was cooled and diluted by distilled water and then filtrated. The product (MWCNTs-COOH) was washed by distilled water and dried at 70 °C for 1 day under reduced pressure. Subsequently, in a 50 mL flask with a magnetic stirring bar, the obtained carboxylated MWCNTs (0.5 g) was dispersed in anhydrous dichloromethane. Then, appropriate quantities of propargyl alcohol and 4-(dimethylamino) pyridine (DMAP) were added to the above mixture. After the flask was cooled to 0 °C, a diluted solution of *N,N'*-dicyclohexyl carbodiimide (DCC) was added dropwise over 2 h. The reaction mixture was warmed to room temperature and stirred for 48 h. The propargyl functionalized MWCNTs obtained from the reaction was separated and washed carefully with methanol, deionised water and again with dry methanol and dried at 50 °C under reduced pressure. The amino-functionalized MWCNTs (MWCNTs-NH₂) was synthesized by “click” reaction between propargyl-functionalized MWCNTs and 3-azidopropylamine. Typically, propargyl-functionalized MWCNTs were dispersed in the mixture of 1:4 (v/v) H₂O and THF by sonication for 10 min, and the reacted with excess of 3-azidopropylamine in the presence of Cu(OAc)₂ and sodium ascorbate catalysts at room

temperature for 48 h. The attachment of amino group onto the MWCNTs was established by FT-IR.

2.4. Preparation of PAMAM-grafted-MWCNTs hybrid materials

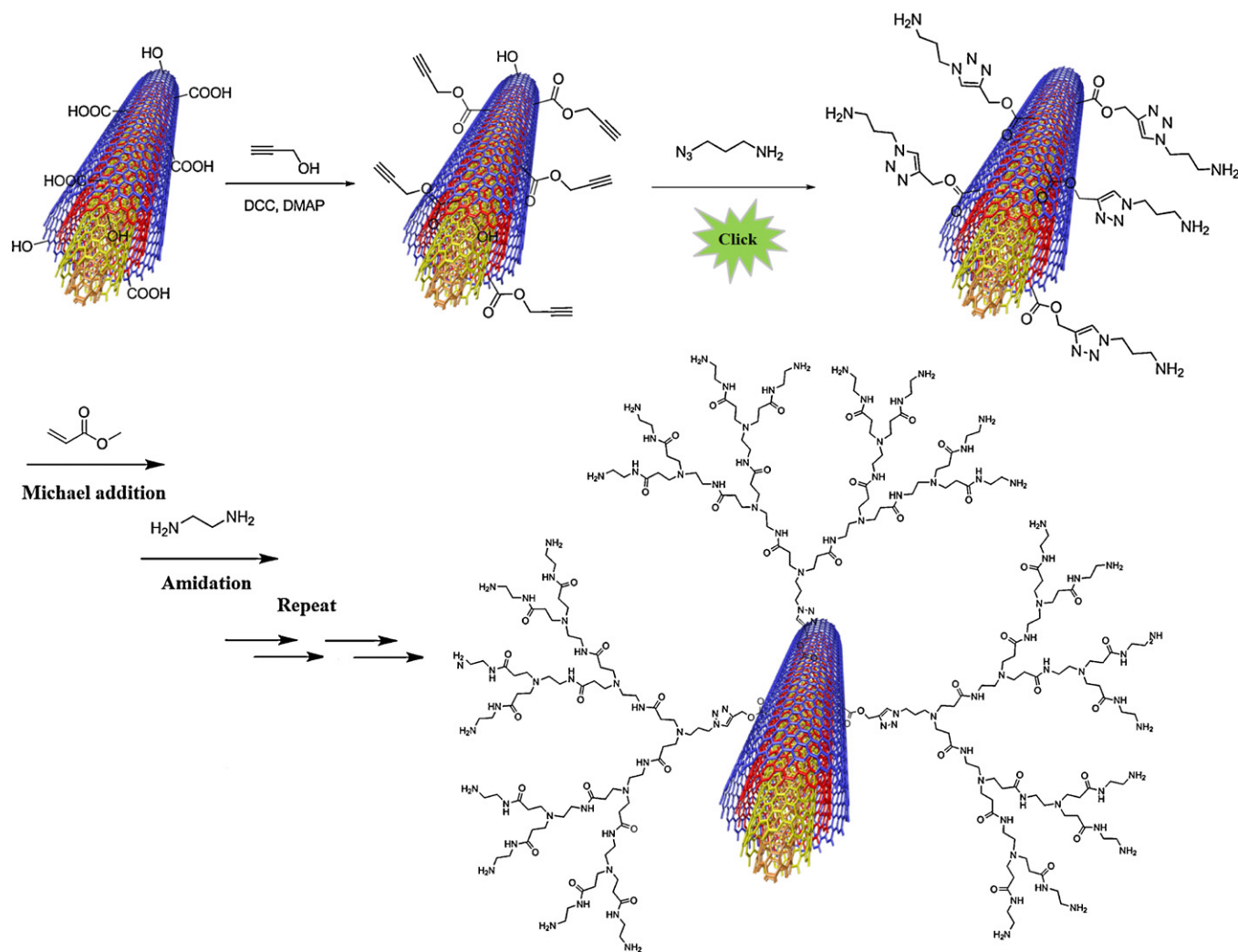
First-, second- and third-generation PAMAM dendrimers were synthesized on the amino functionalized MWCNTs. The amino-functionalized MWCNTs (1 g, 0.17 mmol -NH_2 groups) were added in portions at ambient temperature with stirring to methyl acrylate (8.8 mL, 100 mmol) and methanol (10 mL) in a 100-mL round-bottomed flask. The reaction mixture was stirred at ambient temperature under nitrogen atmosphere for 5 day. After the reaction, excess reactants and solvent were removed under vacuum. The ester-functionalized MWCNTs were washed with methanol, dichloromethane and acetone (3 mL \times 20 mL). It was dried under vacuum for 24 h. Then, the ester-functionalized MWCNTs were added in small fractions with stirring to a mixture of ethylenediamine (6.4 mL, 100 mmol) and methanol (20 mL) in a round-bottomed flask and then cooled to 0 °C in an ice-salt bath. The reaction mixture was stirred at 0 °C for 1 h, the temperature was allowed to rise to ambient temperature, and the mixture was stirred at ambient temperature for 4 day to ensure reaction completion. It was filtered under vacuum, washed with methanol, acetone and diethyl ether (3 mL \times 20 mL) and dried under vacuum for 24 h. Repetition of the above steps gave second- and third-generation PAMAM dendrimers attached on the surface of MWCNTs. After the synthesis, titration method [63] was used to calculate the amount of free primary amines in the periphery of the dendrimers (Table 1). Typically, 0.2 g of PAMAM-grafted-MWCNTs hybrid materials was suspended in 40 mL of 0.01 mol L⁻¹ HCl aqueous solution and stirred at ambient temperature for 24 h. The hybrid materials was filtered and washed well with distilled water. The filtrate and washings were collected. The unreacted HCl was determined by titration against a standard Na₂CO₃ solution with use of methyl orange indicator. A blank titration was also carried out. From these values, the amount of amino groups per gram of the hybrid materials was calculated.

2.5. Preparation of PdNs-PAMAM-g-MWCNTs

Aqueous solution of PdCl₂ (0.26 g in 3 mL) and PAMAM-grafted-MWCNTs (0.2 g in 10 mL) were mixed and placed in an ultrasonic bath (50 KHz) for 10 min to well disperse metal ions in the dendritic shell of hybrid material. Mixture was stirred at room temperature for 8 h and the reduction was carry out by the addition 0.08 mL of aqueous solution of NaBH₄ (0.01 M) to the mixture and stirring at room temperature for 1 h. It was filtered under vacuum, washed well with ethanol and water (2 mL \times 20 mL) and dried under vacuum at 50 °C for 4 h.

2.6. General procedure for the catalytic tests

The coupling reaction was carried out in a glass batch reactor. At first aryl halide (1 mmol) and methyl acrylate or styrene (1 mmol)



Scheme 1. Synthesis route of carbon nanotube-supported poly(amidoamine) dendrimer.

were dissolved in 2 mL NMP. This reactant mixture was then added to the solution of K_2CO_3 (1.2 mmol) in 1 mL of NMP under stirring condition. To this 0.3 mol% of Pd(0) nanocatalyst (PdNs-PAMAM-g-MWCNTs) was added and the reaction mixture was heated to $100^\circ C$ in an oil bath. The reaction was monitored by TLC (or GC if necessary). On completion of the reaction, the mixture was filtered and the filtrate poured into water and extracted with CH_2Cl_2 . The combined organic phases were dried over Na_2SO_4 , filtered and evaporated in vacuum. The mixture was then purified by column chromatography over silica-gel or recrystallization to afford a product with high purity. Characterizations of the products were performed by comparison of their FT-IR, 1H -NMR, ^{13}C -NMR and physical data with those of authentic samples.

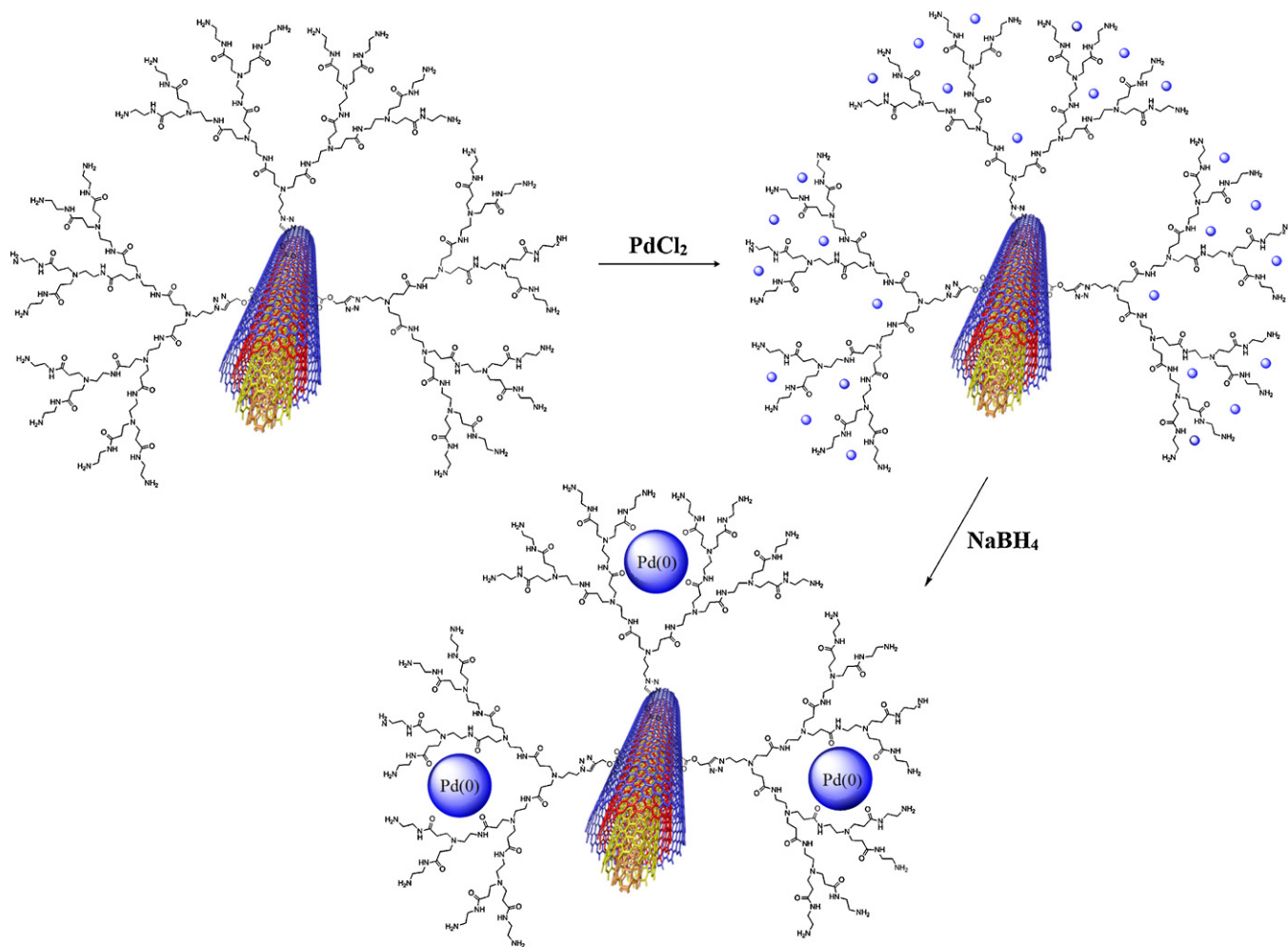
3. Results and discussion

3.1. Synthesis and characterization of the supported catalyst

The chemical modification of MWCNTs and subsequent loading of palladium has been outlined in Schemes 1 and 2. First, the amine-functionalized MWCNTs were obtained using a simple two-step reaction sequence. Consequently, the PAMAM dendrimers up to third generation were grown on the surface of MWCNTs to obtain the PAMAM-grafted-MWCNTs hybrid materials employing a

divergent route starting from the amine-functionalized MWCNTs. A Michael type addition reaction took place between the pre-existing amino groups and the methyl acrylates with the ratio of two propionate ester groups to one amino group. Subsequent ester groups reacted with ethylenediamine to complete the generation. Repetition of these two steps produced the desired generation of the dendrimers. These processes were monitored with the FT-IR. Fig. 1 shows the FT-IR spectra of each generation of PAMAM-grafted-MWCNTs. The absorption band at 1734 cm^{-1} was attributed to the CO stretching of the ester groups, clearly visible in all half-generation products. When the half-generation products react with ethylenediamine to form the corresponding full generation, the peak at 1732 cm^{-1} disappeared, indicating that the reaction has taken place. The broad band at 3424 cm^{-1} is due to the $-NH_2$ stretching, the peaks at 2922 and 2850 cm^{-1} are assigned to the C-H stretching, the strong bands at 1635 cm^{-1} could be assigned to the C=O stretching of amide groups ($-CONH-$) and the peaks at 1550 cm^{-1} are attributed to the N-H bending of the secondary amide groups. The increase in the relative intensity of the above peaks indicates that the dendrimers were successfully constructed on the surface of MWCNTs.

Also, 1H NMR results provide valuable information on the functional groups in the PAMAM-grafted-MWCNTs samples in D_2O (Fig. 2). For the samples with a higher generation of grafted dendrimer (e.g., PAMAM (G3)-g-MWCNTs), the dendrimer unit signals



Scheme 2. Synthesis route of PdNs-PAMAM-g-MWCNTs hybrid materials.

are very strong because of its excellent solubility in water (Fig. 3). The hydrogen peaks of the grafted dendritic units are clearly observed in the corresponding ^1H NMR spectrum [64,65].

Fig. 3 shows the dependence of the solubility on the chemical treatment of the MWCNTs. The dispersion of PAMAM (G3)-g-MWCNTs was stable for at least two days. However, the dispersion of PdNs-PAMAM (G3)-g-MWCNTs gave rise to some precipitates

after two days, which may be due to the high loading of Pd NPs in the hybrid of PdNs-PAMAM-g-MWCNTs.

In addition to the titration method the thermogravimetric analysis (TGA) data were used for the quantification of the growth of the dendrimers on the surface (Fig. 4). The actual weight loss corresponding to the combustion of supported dendrimers was

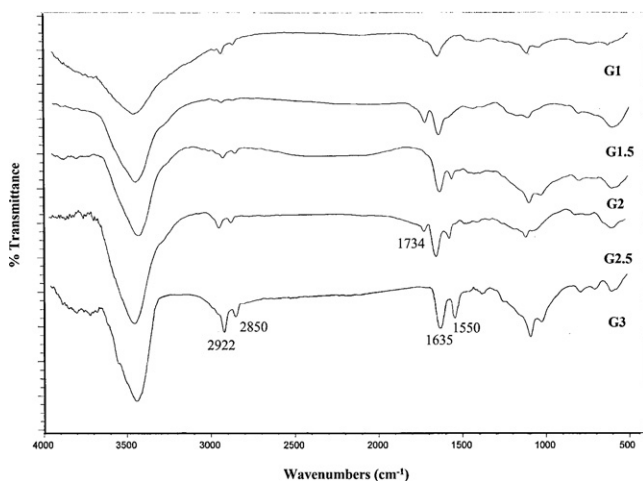


Fig. 1. FT-IR spectra for carbon nanotube-supported dendrimers.

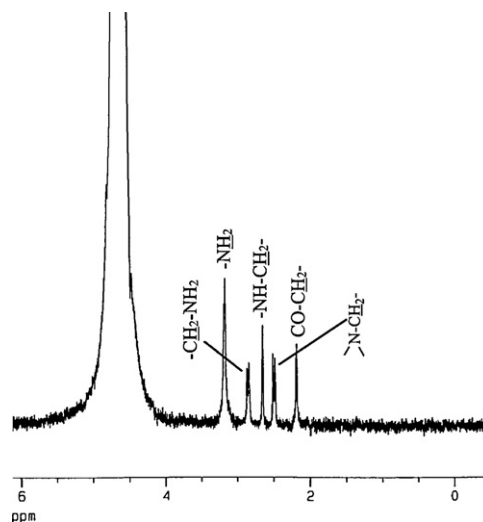


Fig. 2. ^1H -NMR spectrum of carbon nanotube-supported dendrimer (G3) in D_2O .

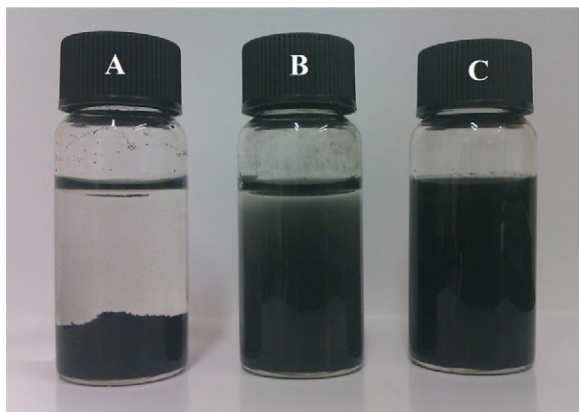


Fig. 3. Comparison of the solubility of (A) MWCNTs, (B) PdNs-PAMAM (G3)-g-MWCNTs and (C) PAMAM (G3)-g-MWCNTs in water.

determined by thermogravimetry as the weight loss between 121 and 700 °C, i.e., excluding the weight loss due to the desorption of water. This value was further corrected for the weight loss due to the amount of MWCNTs in the sample by using the weight loss of the unmodified MWCNTs support. It is interesting to note that the calculated amount of $-NH_2$ groups on each generation of the PAMAM-g-MWCNTs hybrid materials by thermogravimetric analysis was in good agreement with titration-derived amount (Table 1).

In the final step, Pd^{2+} ions were introduced into the dendrimers on the surface of MWCNTs and they were subsequently reduced by sodium borohydride, resulting to the formation of black powders of PdNs-PAMAM-g-MWCNTs. The palladium amounts of every kind of catalyst (G0–G3) were determined by atomic absorption spectroscopy (AAS). The amounts of amino groups and Pd(0) on each generation of the grafted dendrimer are given in Table 1. This data clearly indicate that the loading of metal nanoparticles increases with the increase in the generation of the dendrimer. This can be attributed to an exponential increase of amino groups with the increase in the generation of dendrimer.

TEM experiments demonstrate that palladium nanoparticles were uniformly dispersed on the surface of MWCNTs (Fig. 5A). This is due to the existence of a large number of amine groups, as anchoring sites, on the surface of MWCNTs. Fig. 5B shows the size distribution of encapsulated palladium nanoparticles in the dendritic shell of PAMAM-g-MWCNTs. We found that the main average

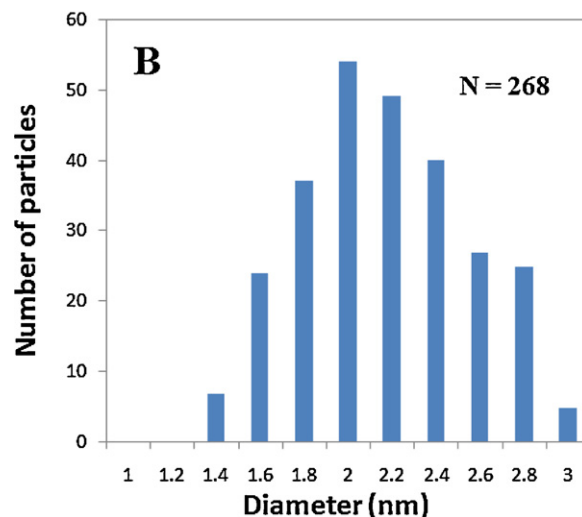
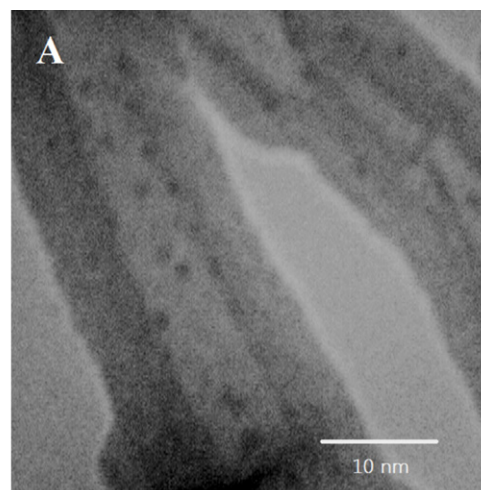


Fig. 5. (A) TEM images of PdNs-PAMAM (G3)-g-MWCNTs and (B) the size distribution of immobilized palladium nanoparticles (N in histogram denotes the counted number of PdNs).

size is around 1.8–2.8 nm and the size distribution is relatively narrow.

X-ray photoelectron spectroscopy (XPS) is a powerful tool for the investigation of CNT-based hybrid materials. Wide XPS scan from PdNs-PAMAM-g-MWCNTs before reaction and after cycle use (Fig. 6A and B) shows the presence of palladium (Pd 3d) together with carbon (C 1s) derived from PAMAM-g-MWCNTs. The nitrogen (N 1s) and oxygen (O 1s) signals are due to PAMAM produced during the synthesis of PdNs-PAMAM-g-MWCNTs hybrid materials. Thus, the XPS data also confirm the presence of Pd in the hybrid materials.

The spectrum of the Pd 3d core level of the Pd-immobilized PAMAM-g-MWCNTs is illustrated in Fig. 7 which reveals the presence of Pd $3d_{5/2}$ and $3d_{3/2}$ peaks at binding energies of 335.5 and 340.85 eV, respectively. These binding energy values are in accordance with those reported for metallic Pd(0) oxidation state [66]. Additionally, it is worth stressing that no significant traces of oxidized Pd are present: indeed, PdO would appear at a higher BE shoulder approximately 1.5–2.0 eV away from the Pd(0) peak [66].

The XRD patterns for the nanocatalyst show the expected crystallinity of Pd(0) nanoparticles and amorphous MWCNTs (Fig. 8). The broad peaks at $2\theta = 26.28^\circ$ are associated with the (002) planes of the graphite like structure of the multi-walled carbon nanotubes [67]. The other three peaks of PdNs-PAMAM-g-MWCNTs are characteristic of face centered cubic (fcc) crystalline Pd, corresponding

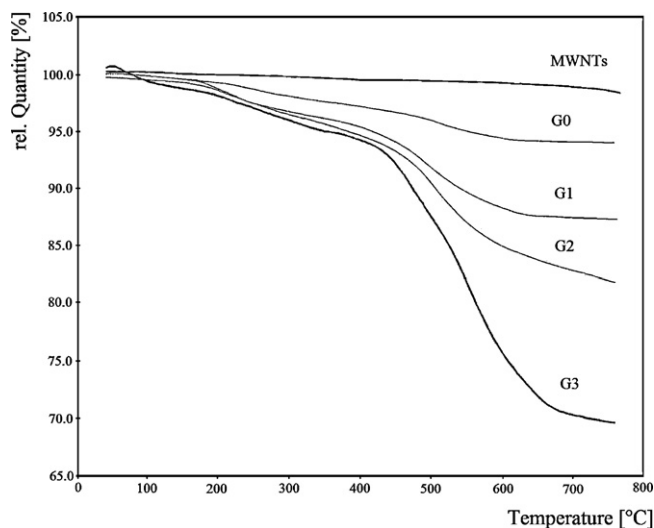


Fig. 4. Weight loss as measured by TGA for MWNTs-supported dendrimers.

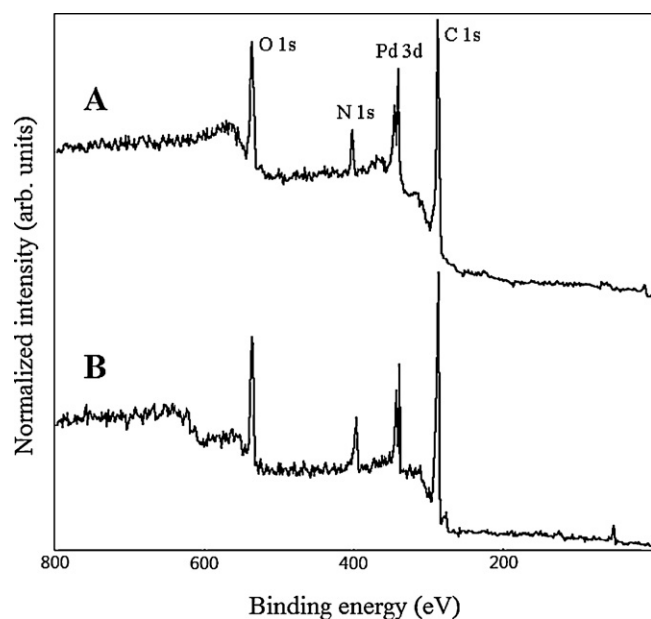


Fig. 6. Wide XPS scan of PdNs-PAMAM (G3)-g-MWCNTs hybrid material (A) before reaction and (B) after cycle use.

to the planes (1 1 1), (2 0 0) and (2 2 0) at 2θ values of about 40.02, 46.59, and 68.03, respectively. The same result was also obtained for the XRD pattern of the catalyst after its use in the Heck reaction for several cycles. This reveals the excellent stability and recovery of the catalyst.

3.2. The catalytic activity of PdNs-PAMAM-g-MWCNTs toward the Heck cross-coupling reactions

To evaluate the catalytic properties of these catalysts, Heck coupling reaction of 4-methyl-iodobenzene with methyl acrylate was performed as a model reaction. Initially, the reaction was carried out in the presence of various amounts of catalyst in *N*-methylpyrrolidone (NMP) (Table 2). At very low catalyst loading, the reaction required long duration to get completed even under harsh thermal conditions (130 °C). As the catalyst amount was increased (0.3 mol% with respect to 4-methyl-iodobenzene), the reaction went to completion more rapidly at 100 °C. Since the amount of catalyst and the reaction temperature were optimized, the influence of solvent and base on the reaction was studied in the next step (Tables 3 and 4). It was found that the best system

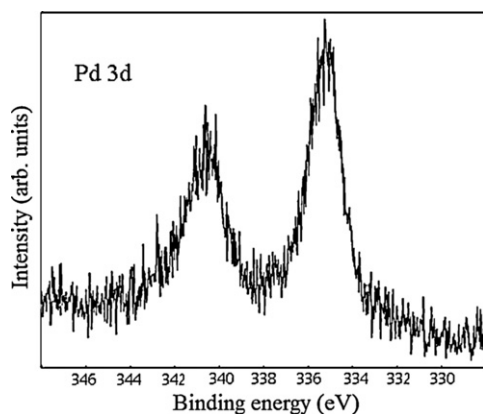


Fig. 7. X-ray photoemission spectra of the Pd 3d core level region for PdNs-PAMAM (G3)-g-MWCNTs hybrid material.

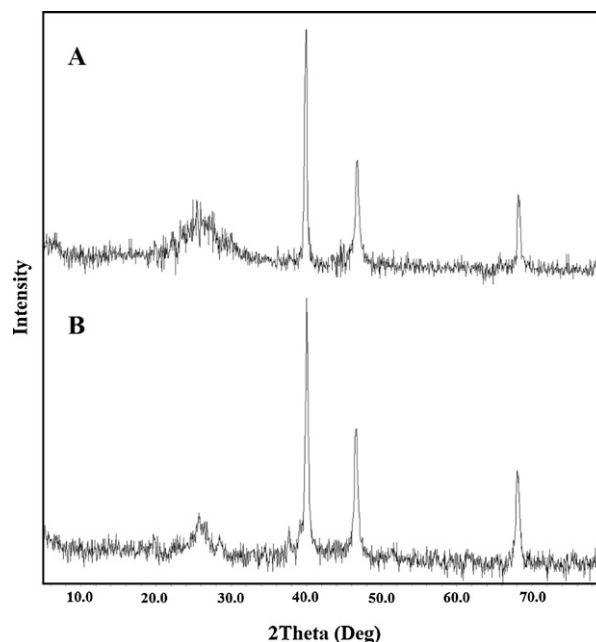


Fig. 8. X-ray diffraction (XRD) pattern of PdNs-PAMAM (G3)-g-MWCNTs hybrid material (A) before reaction and (B) after cycle use.

Table 2

Influence of the amount of catalyst on Heck coupling reaction of 4-methyl-iodobenzene with methyl acrylate.^a

Entry	Amount of catalyst (Pd(0) content/mol%)	Temp (°C)	Conversion (%)
1	0.1	130	46
2	0.1	100	37
3	0.2	100	75
4	0.3	100	99 (45 ^b , 78 ^c)
5	0.5	100	99 (57 ^b , 80 ^c)

^a Reaction conditions: 1 mmol 4-methyl-iodobenzene, 1 mmol methyl acrylate, 1.2 mmol K₂CO₃, 3 mL NMP, PdNs-PAMAM (G3)-g-MWCNTs as catalyst, 2 h.

^b Conversion after 0.5 h.

^c Conversion after 1 h.

Table 3

Effect of different bases on the reaction of 4-methyl-iodobenzene and methyl acrylate.^a

Entry	Base	Conversion (%)
1	None	Trace
2	Et ₃ N	99 (40 ^b , 75 ^c)
3	K ₂ CO ₃	99 (45 ^b , 78 ^c)
4	NaOAc	85
5	CsCO ₃	68

^a Reaction conditions: 1 mmol 4-methyl-iodobenzene, 1 mmol methyl acrylate, 100 °C, base 1.2 mmol, 3 mL NMP, PdNs-PAMAM (G3)-g-MWCNTs (Pd(0) content/0.3 mol%) as catalyst, 2 h.

^b Conversion after 0.5 h.

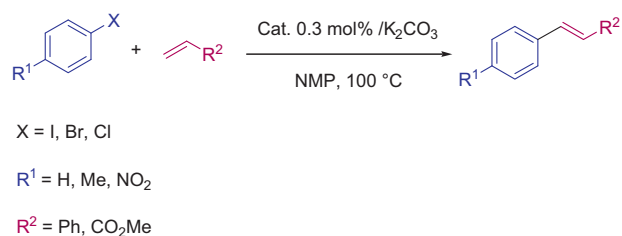
^c Conversion after 1 h.

Table 4

Effect of different solvents on the reaction of 4-methyl-iodobenzene and methyl acrylate.^a

Entry	Solvent	Time (h)	Conversion (%)
1	DMF	2	90
2	THF	5	24
3	CH ₃ CN	5	30
4	Toluene	5	33
5	H ₂ O	5	50
6	NMP	2	99

^a Reaction conditions: 1 mmol 4-methyl-iodobenzene, 1 mmol methyl acrylate, 1.2 mmol K₂CO₃, 100 °C, PdNs-PAMAM (G3)-g-MWCNTs (Pd(0) content/0.3 mol%) as catalyst.



Scheme 3. Mizoroki–Heck cross-coupling reactions.

was NMP as solvent and K₂CO₃ or Et₃N as base using 0.3 mol% of catalyst at 100 °C.

In order to prove the efficiency of the catalyst, we studied the Heck coupling reaction of styrene and methyl acrylate with different aryl halides under similar conditions (Scheme 3 and Table 5). The results show that aryl halides with either electron-withdrawing or electron-donating substituents react with olefins rapidly and generate the coupled products with excellent yields. The coupling reactions with methyl acrylate as the olefin were faster than styrene. The aryl chlorides as readily available and industrially important compounds have not been employed much in palladium-catalyzed coupling reactions primarily because the oxidative addition of C–Cl bond to Pd(0) species is usually difficult.

Table 6
Effect of dendrimer generation on catalysis.^a

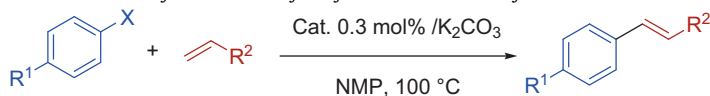
Entry	Generation	Conversion (%)
1	0	50
2	1	74
3	2	87
4	3	99

^a Reaction conditions: 1 mmol 4-methyl-iodobenzene, 1 mmol methyl acrylate, 1.2 mmol K₂CO₃, 100 °C, catalyst (Pd(0) content/0.3 mol%), 2 h.

Few heterogeneous Pd catalysts were found to convert activated aryl chlorides at high temperatures [68–70]. Furthermore, as shown in Table 5 (entries 11–16) the catalytic amount of PdNs-PAMAM (G3)-g-MWCNTs can be used in the Heck coupling of even less reactive aryl chloride derivatives with olefins in good yields.

As the generation of the dendrimer increases, the stability and catalytic efficiency of the PdNs-PAMAM-g-MWCNTs catalyst also increase (Table 6). This result can be explained if we consider that with the increase in generation, the dendrimer has a more closed template preventing the metal nanoparticles leaching and thereby increases the stability of the catalyst. Also, the dendrimer acts as a linker between the support and the catalytic site reducing the steric factors offered by the support to some extent. This effect was

Table 5
Heck reaction of styrene and methyl acrylate with different aryl halides.^a



Entry	ArX	R ²	Time (h)	Yield (%) ^b
1		Ph	2.5	95
2		CO ₂ Me	1	95
3		Ph	3	93
4		CO ₂ Me	2	95
5		Ph	3	88
6		CO ₂ Me	2	90
7		Ph	3.5	90
8		CO ₂ Me	2.5	92
9		Ph	2	93
10		CO ₂ Me	0.5	95
11		Ph	6	65
12		CO ₂ Me	4	80
13		Ph	7	60
14		CO ₂ Me	5	72
15		Ph	2	88
16		CO ₂ Me	1	92

^a Reaction conditions: 1 mmol ArX, 1 mmol Olefin, 1.2 mmol K₂CO₃, 100 °C, PdNs-PAMAM (G3)-g-MWCNTs (Pd(0) content/0.3 mol%) as catalyst.

^b Isolated yield of pure product.

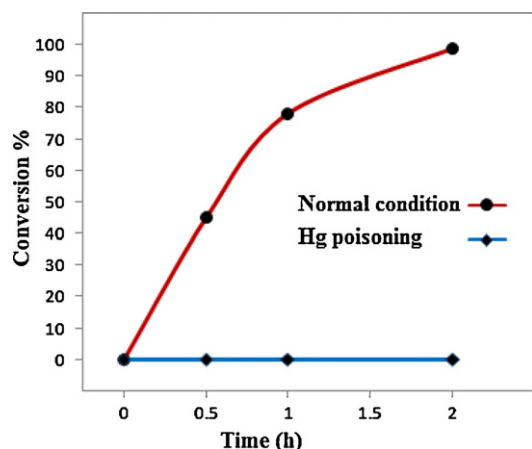


Fig. 9. Kinetic profiles for the coupling of 4-methyl-iodobenzene to methyl acrylate under normal conditions and in presence of excess Hg(0).

high in third generation dendrimers and so they perform as better catalysts compared to the lower generations.

To determine Pd(0) as the active site of the PdNs-PAMAM-g-MWCNTs, Hg(0) poisoning test was done [71]. To perform the test, 0.1 mL (1.35 g) of mercury was added to 3 mL of NMP along with 0.0015 g (Pd(0) content, 0.3 mol%) of PdNs-PAMAM (G3)-g-MWCNTs, and the mixture was stirred for 12 h at room temperature. To this, 1 mmol of 4-methyl-iodobenzene, 1 mmol of methyl acrylate, and 1.2 mmol of K_2CO_3 were added. The mixture was then heated up to 100 °C in an oil bath. The progress of the reactions was monitored by the method described in Section 2. The catalyst was found to be totally inactive toward the coupling reaction in this condition (Fig. 9). This shows that the metallic mercury amalgamates with Pd(0), thereby quenching the activity of the Pd(0) particles that catalyze the Heck reactions.

The lifetime and leaching of active metal species into solution are important issues to be considered when heterogeneous catalysts are used. To address these issues, we have undertaken a series of tests as described below.

Our preliminary investigations demonstrate that catalyst PdNs-PAMAM (G3)-g-MWCNTs is very stable to air and moisture. Moreover, in a separate experiment the catalyst was filtered off after ~50% conversion at the reaction temperature. Further treatment of the filtrate under similar reaction condition did not proceed significantly. On the other hand, atomic absorption spectroscopy of the filtrate also confirmed that the Pd content in the solution was below the detection limit (0.1 ppm). Therefore, we may conclude that any palladium species that leaches into the reaction mixture are not active homogeneous catalysts and that the observed catalysis is truly heterogeneous in nature.

It has been proved that the solid-phase poisoning test is the most definitive test available to date to ascertain the true heterogeneity of the Pd-based catalyst in C–C coupling reactions [72]. In this test, metal-free mercaptopropyl-functionalized silica was used as an effective palladium scavenger that selectively coordinates and deactivates the leached out palladium. Thereby, cessation of the reaction is expected if catalysis of the coupling reaction catalyzed by leached palladium species from the solid support. We have performed solid-phase poisoning tests varying the S/Pd ratio from 5:1 to 500:1 for Heck reaction using commercially available 3-mercaptopropyl-functionalized silica (SH-SiO₂) as poisoning agent. Appropriate amounts of PdNs-PAMAM (G3)-g-MWCNTs and SH-SiO₂ were taken in the solution of 4-methyl-iodobenzene (1 mmol), methyl acrylate (1 mmol), and K_2CO_3 (1.2 mmol) in 3 mL of NMP. The mixture was stirred continuously maintaining the desired temperature. The progress of the reactions was monitored

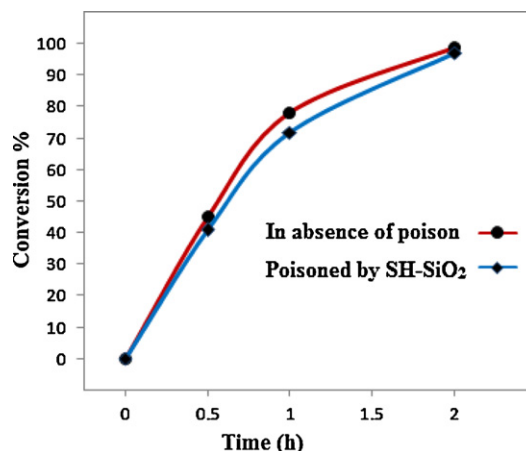


Fig. 10. Kinetic profiles for the coupling of 4-methyl-iodobenzene to methyl acrylate in the absence of solid-phase poison and in the presence of SH-SiO₂ as the solid-phase poison.

Table 7

Effect of recycling on the catalytic efficiency of PdNs-PAMAM (G3)-g-MWCNTs.^a

No. of recycling steps	Conversion (%)
1	99
2	99
3	98
4	98
5	97
6	95

^a Reaction conditions: 1 mmol 4-methyl-iodobenzene, 1 mmol methyl acrylate, 1.2 mmol K_2CO_3 , 100 °C, PdNs-PAMAM (G3)-g-MWCNTs (Pd(0) content/0.3 mol%) as catalyst, 2 h.

by the method described in Section 2. A comparison of the percentage of conversion in C–C coupling reactions clearly shows that the catalytic efficacy of PdNs-PAMAM (G3)-g-MWCNTs is not affected when SH-SiO₂ is added to the reaction mixture. The kinetic profiles of the typical Heck reactions in presence of the poisoning agent SH-SiO₂ (sulfur to palladium ratio; 500/1) are shown in Fig. 10. Notably there was no induction period in these reactions in the presence or in absence of the poisoning agent. Therefore, the above test convincingly demonstrates that there was no leaching of Pd species occurring in PdNs-PAMAM (G3)-g-MWCNTs catalyzed C–C coupling reactions.

The recyclability and reusability of the PdNs-PAMAM (G3)-g-MWCNTs catalyst was tested for the Heck coupling reaction of 4-methyl-iodobenzene with methyl acrylate up to six cycles. The results shown in Table 7 demonstrate that after every run, the yield of product does not change indicating the fair stability of catalyst under experimental conditions. The estimated turn over number (TON = mole of product/mole of catalyst) is calculated to be 1948 for the whole recycling processes.

4. Conclusion

In conclusion, PAMAM dendrimers up to the third generation were grown onto the surface of functionalized multiwall carbon nanotubes by a divergent method. Detailed characterization using ¹H-NMR, FT-IR, XPS, TEM and thermogravimetry analysis show that the dendrimers form onto the surface of the multiwall carbon nanotubes. The PAMAM-g-MWCNTs hybrid materials were effectively employed as substrate for in situ generation of Pd nanoparticles. The deposition of Pd nanoparticles on PAMAM-g-MWCNTs was confirmatively studied by AAS, XPS, XRD and TEM. These hybrid materials were found to be efficient and reusable catalysts in

cross-coupling reactions of aryl iodides, bromides and also chlorides with olefinic compounds in Heck reactions in short reaction time and high yields. The catalysts remain stable under different reaction conditions and with various substrates. The stability and catalytic activity was higher for the third generation dendrimer-based catalyst. Further efforts to extend the application of this system in other reactions are currently in progress in our laboratory.

Acknowledgements

We are grateful to Shahid Beheshti University Research Council for partial financial support of this work.

References

- [1] S. Iijima, *Nature* 354 (1991) 56–58.
- [2] R.H. Baughman, A.A. Zakhidov, W.A. de Heer, *Science* 297 (2002) 787–792.
- [3] J. Gooding, *J. Electrochim. Acta* 50 (2005) 3049–3060.
- [4] S.M. Chergui, A. Ledebt, F. Mammeri, F. Herbst, B. Carbonnier, H.B. Romdhane, M. Delamar, M.M. Chehimi, *Langmuir* 26 (2010) 16115–16121.
- [5] S. Song, H. Yang, R. Rao, H. Liu, A. Zhang, *Appl. Catal. A: Gen.* 375 (2010) 265–271.
- [6] C. Burda, X.B. Chen, R. Narayanan, M.A. El-Sayed, *Chem. Rev.* 105 (2005) 1025–1102.
- [7] G.R. Krishnan, K. Sreekumar, *Appl. Catal. A: Gen.* 353 (2009) 80–86.
- [8] G.R. Krishnan, K. Sreekumar, *Eur. J. Org. Chem.* (2008) 4763–4768.
- [9] T. Maiyalagan, *J. Solid State Electrochem.* 13 (2009) 1561–1566.
- [10] Y. Jiang, J. Jiang, Q. Gao, M. Ruan, H. Yu, L. Qi, *Nanotechnology* 19 (2008) 075714.
- [11] H. Hagiwara, H. Sasaki, N. Tsubokawa, T. Hoshi, T. Suzuki, T. Tsuda, S. Kuwabata, *Synlett* (2010) 1990–1996.
- [12] J.P.K. Reynhardt, Y. Yang, A. Sayari, H. Alper, *Chem. Mater.* 16 (2004) 4095–4102.
- [13] X. Lu, T. Imae, *J. Phys. Chem. C* 111 (2007) 8459–8462.
- [14] S.H. Hwang, C.N. Moorefield, P. Wang, K.U. Jeong, S.Z.D. Cheng, K.K. Kotta, G.R. Newkome, *J. Am. Chem. Soc.* 128 (2006) 7505–7509.
- [15] M. Adeli, E. Mehdipour, M. Bavadi, *J. Appl. Polym. Sci.* 116 (2010) 2188–2196.
- [16] Y. Jiang, Q. Gao, *J. Am. Chem. Soc.* 128 (2006) 716–717.
- [17] D.A. Tomalia, J.M.J. Frechet, in: D.A. Tomalia, J.M.J. Frechet (Eds.), *Dendrimers and Other Dendritic Polymers*, John Wiley & Sons, Ltd, UK, 2001, pp. 3–44.
- [18] C.J. Hawker, J.M.J. Frechet, *J. Chem. Soc. Chem. Commun.* (1990) 1010–1013.
- [19] D.A. Tomalia, H. Baker, J.R. Dewald, M. Hall, G. Kallos, S. Martin, J. Roeck, J. Ryder, P. Smith, *Polym. J.* 17 (1985) 117–132.
- [20] Q. Feng, X.M. Xie, Y.T. Liu, W. Zhao, Y.F. Gao, *J. Appl. Polym. Sci.* 106 (2007) 2413–2421.
- [21] S.M. Grayson, J.M.J. Frechet, *Chem. Rev.* 101 (2001) 3819–3867.
- [22] S. Qin, D. Qin, W.T. Ford, D.E. Resasco, J.E. Herrera, *J. Am. Chem. Soc.* 126 (2004) 170–176.
- [23] N.R. Shiju, V.V. Gulians, *Appl. Catal. A: Gen.* 356 (2009) 1–17.
- [24] R. Narayanan, *Molecules* 15 (2010) 2124–2138.
- [25] S. Cheong, J.D. Watt, R.D. Tilley, *Nanoscale* 2 (2010) 2045–2053.
- [26] L. Xue, Z. Lin, *Chem. Soc. Rev.* 39 (2010) 1692–1705.
- [27] G.A. Molander, B. Canturk, *Angew. Chem. Int. Ed.* 48 (2009) 9240–9261.
- [28] N. Miyaura, A. Suzuki, *Chem. Rev.* 95 (1995) 2457–2483.
- [29] C. Amatore, A. Jutand, *Acc. Chem. Res.* 33 (2000) 314–321.
- [30] K.C. Nicolaou, P.G. Bulger, D. Sarlah, *Angew. Chem. Int. Ed.* 44 (2005) 4442–4489.
- [31] B. Schlummer, U. Scholz, *Adv. Synth. Catal.* 346 (2004) 1599–1626.
- [32] M. Lamblin, L. Nassar-Hardy, J.C. Hierso, E. Fouquet, F.X. Felpin, *Adv. Synth. Catal.* 352 (2010) 33–79.
- [33] L. Yin, J. Liebscher, *Chem. Rev.* 107 (2007) 133–173.
- [34] J.Y. Kim, Y. Jo, S.K. Kook, S. Lee, H.C. Choi, *J. Mol. Catal. A: Chem.* 323 (2010) 28–32.
- [35] S.A. Patel, K.N. Patel, S. Sinha, B.V. Kamath, A.V. Bedekar, *J. Mol. Catal. A: Chem.* 332 (2010) 70–75.
- [36] B.C.E. Makhubela, A. Jardine, G.S. Smith, *Appl. Catal. A: Gen.* 393 (2011) 231–241.
- [37] B. Tamami, H. Allahyari, S. Ghasemi, F. Farjadian, *J. Organomet. Chem.* 696 (2011) 594–599.
- [38] Y. Zhao, X. Yang, J. Tian, F. Wang, L. Zhan, *Mater. Sci. Eng. B* 171 (2010) 109–115.
- [39] N. Karousis, G.E. Tsotsou, F. Evangelista, P. Rudolf, N. Ragoussis, N. Tagmatarchis, *J. Phys. Chem. C* 112 (2008) 13463–13469.
- [40] S. Bhunia, R. Sen, S. Koner, *Inorg. Chim. Acta* 363 (2010) 3993–3999.
- [41] J. Guerra, M.A. Herrero, *Nanoscale* 2 (2010) 1390–1400.
- [42] T. Borkowski, A.M. Trzeciak, W. Bukowski, A. Bukowska, W. Tylus, L. Kepinski, *Appl. Catal. A: Gen.* 378 (2010) 83–89.
- [43] F. Durap, M. Rakap, M. Aydemir, S. Ozkar, *Appl. Catal. A: Gen.* 382 (2010) 339–344.
- [44] Y. He, C. Cai, *Catal. Commun.* 12 (2011) 678–683.
- [45] A. Villa, D. Wang, N. Dimitratos, D. Su, V. Trevisan, L. Prati, *Catal. Today* 150 (2010) 8–15.
- [46] Y.S. Chun, J.Y. Shin, C.E. Song, S. Lee, *Chem. Commun.* (2008) 942–944.
- [47] S. Ungureanu, H. Deleuzeb, O. Babotb, M.F. Acharda, C. Sanchez, M.I. Popad, R. Backov, *Appl. Catal. A: Gen.* 390 (2010) 51–58.
- [48] S.M. Islam, P. Mondal, K. Tuhina, A.S. Roy, S. Mondal, D. Hossain, *J. Inorg. Organomet. Polym.* 20 (2010) 264–277.
- [49] Z. Gao, Y. Feng, F. Cuia, Z. Huua, J. Zhoua, Y. Zhua, J. Shi, *J. Mol. Catal. A: Chem.* 336 (2011) 51–57.
- [50] S.M. Islam, P. Mondal, K. Tuhina, A.S. Roy, S. Mondal, D. Hossain, *J. Organomet. Chem.* 695 (2010) 2284–2295.
- [51] R.U. Islam, M.J. Witcomb, E. Lingen, M.S. Scurrill, W.V. Otterlo, K. Mallick, *J. Organomet. Chem.* 696 (2011) 2206–2210.
- [52] D.H. Lee, J.Y. Jung, M.J. Jin, *Green Chem.* 12 (2010) 2024–2029.
- [53] C.M. Cirtiu, A.F. Dunlop-Briere, A. Moores, *Green Chem.* 13 (2011) 288–291.
- [54] X. Chen, Y. Hou, H. Wang, Y. Cao, J. He, *J. Phys. Chem. C* 112 (2008) 8172–8176.
- [55] J. Zhu, J. Zhou, T. Zhao, X. Zhou, D. Chen, W. Yuan, *Appl. Catal. A: Gen.* 352 (2009) 243–250.
- [56] S. Wu, H. Ma, X. Jia, Y. Zhong, Z. Lei, *Tetrahedron* 67 (2011) 250–256.
- [57] S.M. Islam, P. Mondal, K. Tuhina, A.S. Roy, *J. Chem. Technol. Biotechnol.* 85 (2010) 999–1010.
- [58] M.R. Nabid, R. Sedghi, P.R. Jamaat, N. Safari, A.A. Entezami, *Appl. Catal. A: Gen.* 328 (2007) 52–57.
- [59] M.R. Nabid, S.J. Tabatabaei Rezaei, *Appl. Catal. A: Gen.* 366 (2009) 108–113.
- [60] M.R. Nabid, S.J. Tabatabaei Rezaei, S.Z. Hosseini, M. Abedi, *Synth. Commun.*, in press.
- [61] M.R. Nabid, S.J. Tabatabaei Rezaei, M. Abedi, *Synth. Commun.* 41 (2011) 191–199.
- [62] X. Jiang, J. Zhang, Y. Zhou, J. Xu, S. Liu, *J. Polym. Sci. Part A: Polym. Chem.* 46 (2008) 860–871.
- [63] M.P. Kapoor, Y. Kasama, T. Yokoyama, M. Yanagi, S. Inagaki, H. Nanbu, L.R. Juneja, *J. Mater. Chem.* 16 (2006) 4714–4722.
- [64] J.W. Lee, J.H. Kim, B.K. Kim, J.H. Kim, W.S. Shin, S.H. Jin, *Tetrahedron* 62 (2006) 9193–9200.
- [65] B. Pan, D. Cui, F. Gao, R. He, *Nanotechnology* 17 (2006) 2483–2489.
- [66] H.-G. Boyen, P. Ziemann, U. Wiedwald, V. Ivanova, D.M. Kolb, S. Saking, A. Gross, A. Romanyuk, M. Buttner, P. Oelhafen, *Nat. Mater.* 5 (2006) 394–399.
- [67] G. Guo, F. Qin, D. Yang, C. Wang, H. Xu, S. Yang, *Chem. Mater.* 20 (2008) 2291–2297.
- [68] K. Selvakumar, A. Zapf, M. Beller, *Org. Lett.* 4 (2002) 3031–3033.
- [69] S. Prockl, W. Kleist, M.A. Gruber, K. Kohler, *Angew. Chem. Int. Ed.* 43 (2004) 1917–1918.
- [70] K. Kohler, W. Kleist, S.S. Prockl, *Inorg. Chem.* 46 (2007) 1876–1883.
- [71] K. Yu, W. Sommer, J.M. Richardson, M. Weck, C.W. Jones, *Adv. Synth. Catal.* 347 (2005) 161–171.
- [72] J.M. Richardson, C.W. Jones, *J. Catal.* 251 (2007) 80–93.